

Power Over Fiber in C-RAN With Low Power Sleep Mode Remote Nodes Using SMF

Juan Dayron López-Cardona , Rubén Altuna , David Sánchez Montero ,
and Carmen Vázquez , *Senior Member, IEEE*

Abstract—Power over fiber (PoF) with sleep mode operation in centralized radio access networks (C-RAN) of low power Remote Radio Heads (RRH) helps to reduce power consumption. This proposal includes bundles of single mode optical fibers (SMF) as part of the 5G C-RAN front-haul solution for providing control on power consumption by selectively activating some parts of the RRH. We experimentally demonstrate a PoF system based on 14.43 km of SMF feed by 2.24 W giving 226 mW electrical power at the RRH for control, battery charge, load operation and communication purposes. A bidirectional control channel is integrated in the central office and the RRH for providing the capability of entering in sleep mode operation and to provide information about the status of the battery and sensing elements at RRH. The optical data uplink/downlink operates over separate optical fibers shared by various RRHs and achieves low power consumption below 33 mW with low data rates. The measured PV cells conversion efficiency is above 30%. The RRH has two sleep modes of operation with a minimum power consumption of 5.8 mW.

Index Terms—Energy efficiency, high power lasers, photovoltaic cells, power over fiber (PoF), radio access networks (RAN), remote radio heads (RRH), sensors, single mode fiber (SMF), sleep mode, stimulated Raman scattering (SRS).

I. INTRODUCTION

POWER over fiber (PoF) is a good strategy for providing energy to remote points free of electromagnetic interference, with low weight, good galvanic isolation and with an easy integration in the infrastructure of telecommunications operators. Optical fibers are also among the technologies supporting the increasing capacity of 5G radio access networks (RAN), as part of the back/front haul infrastructure for transmitting radio-over-fiber (RoF) signals. The higher bandwidth required on those networks fosters the deployment of a large number of reduced cell sites with the consequent increment of power consumption and cost unless special strategies are considered. The

Manuscript received November 17, 2020; revised March 26, 2021 and April 29, 2021; accepted May 12, 2021. Date of publication May 14, 2021; date of current version August 2, 2021. This work was supported in part by the Spanish Ministerio de Ciencia, Innovación y Universidades, Madrid Government (Comunidad de Madrid-Spain) and H2020 European Union programme under Grants RTI2018-094669-B-C32, Y2018/EMT-4892, P2018/NMT-4326, and 5G PPP Bluespace Project Grant 762055, respectively. (*Corresponding author: Carmen Vázquez.*)

The authors are with Electronics Technology Department, Universidad Carlos III de Madrid, Leganés 28911, Madrid, Spain (e-mail: julopezc@ing.uc3m.es; raltuna@pa.uc3m.es; dsmontero@ing.uc3m.es; cvazquez@ing.uc3m.es).

Color versions of one or more figures in this article are available at <https://doi.org/10.1109/JLT.2021.3080631>.

Digital Object Identifier 10.1109/JLT.2021.3080631

Cloud-RAN or Centralized-RAN (C-RAN) architecture centralizing the computing power allows controlling and simplifying the management of the mobile network [1]. The required remote radio heads (RRH) are simplified, especially when using Analog Radio over Fiber (ARoF) technologies with the consequent reduction in power consumption. As an example a 23.5–31.5 GHz photodetector and co-designed low noise amplifier consuming around 160 mW is reported in [2]. Some authors propose using the capability of turning into sleep mode some RRHs, avoiding current situation with a continuous feeding even with no users in the cell and for providing the maximum traffic load. Improvements of a 40% energy reduction in a whole day using the C-RAN architecture can be achieved [3]. Others proposed switching the energy between different RRHs depending on traffic demand [4] through a Software Defined Network (SDN) controller. Meanwhile there is no hardware demonstration yet of that capability.

A summary about the main achievements in PoF applied to RoF for different types of fibers and commercial products is reported in [5]. Higher PoF power levels are fed using multimode fibers (MMF) and high power lasers (HPL) around 808 nm, one of the first attempts provided 4 W of electrical power using 8 MMFs at 12 m [6]. More recently, double-clad fibers (DCF) are fed with up to 150 W optical power [7] in a 1 km-long link and with a 4.84% optical-to-electrical power transmission efficiency, i.e., from HPL optical power to photovoltaic (PV) converter electrical power. Single mode optical fibers (SMF) provide lower power levels but at higher link lengths being more suitable for C-RAN fronthauls using ARoF for distances around 10 km or more [8], [9] if one considers the use of an already deployed infrastructure to provide control functionalities and partial powering. On the other hand, Spatial Division Multiplexing using multicore fibers (MCF) versus bundles of optical fibers for ARoF transport in combination with PoF is proposed for 5G high-bandwidth fronthauling in the EU H2020 5G-PPP project blueSPACE [10]. Recently, SMFs have been used [11] for feeding with 190 mW electrical power a sensor node located 8 km away in a cabled seafloor observatory. The already installed SMF make it an attractive solution when convergence between wireless and optical access networks is considered.

In this paper, we focus in low and medium power consumption RRHs and their remote control means to improve efficiency using different sleep mode operations. We use bundles of SMFs as part of the 5G C-RAN front-haul solution for providing control on power consumption by selectively activating some

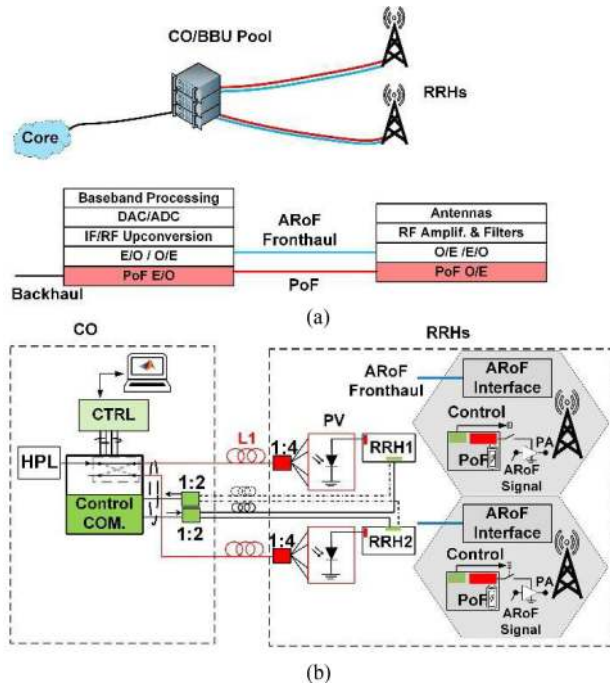


Fig. 1. Schematic of the PoF system: (a) Within C-RAN, (b) Main elements. CO: Central office. BBU: Base band unit. RRH: Remote radio head. ARoF: Analog radio over fiber. HPL: High power laser. PV: Photovoltaic cell. COM: Communications. CTRL: Control. PA: Power amplifier.

parts of the RRH. We experimentally demonstrate a PoF system based on 14.43 km of SMF feed by 2.24 W giving 226 mW electrical power at the RRH for control, battery charge, load operation and communication purposes. A bidirectional control channel is integrated in the central office (CO) and in the RRHs capable of providing sleep mode operation as well as information about the status of the battery and sensing elements inside the RRH. All designs at RRH are low power consumption driven with a minimum power of 5.8 mW in deep sleep mode.

This paper is organized as follows. In Section II, we describe the system configuration integrated in the C-RAN architecture and the main elements. In Section III, we describe the experimental setup for evaluating the performance of the power delivering in a 14.43-km SMF link including communications, control and potential impact of nonlinear effects. We also evaluate the power consumption, sleep mode operation and the different functionalities. Section IV concludes the paper.

II. SYSTEM CONFIGURATION

The developed system consists of a central office (CO) located in the Base Band Units (BBU) pool area of the C-RAN, see Fig. 1(a), a remote receiver unit as part of a RRH and a bidirectional communication between them, meaning adding a PoF layer to the ARoF fronthaul described in [9]. PoF system can feed very low power 5G RRHs or some parts of them. It can also control the feeding of specific parts or make them entering into sleep mode operation, for example by switching the power amplifiers (PA).

The CO includes a HPL, a communication (COM) unit and a control unit, as shown in Fig. 1(b). The RRH has an energy

TABLE I
SYSTEM SPECIFICATIONS

Optical fiber	14.43 km SMF (1 power, 2 uplink/downlink)
HPL	1480 nm Fiber Raman laser up to 5 W
PV cells	4x SMF pigtailed up to 3 V-20 mA output
RRH output voltage	5 V
RRH feeding power	226 mW(electrical)
RRH sleep mode 1	115 mW (electrical)
RRH sleep mode 2	5.8 mW (electrical)

management unit with the PV cells, different regulators (LDO and DC/DC), control and communication units. In the optical plane, there is a bundle of three SMFs. Downlink/uplink communication at 1310 nm use 2 SMFs and a 1×2 splitter for sharing the communication channel between two RRHs (see Fig. 1(b)). Depending on the location of both RRHs in the deployment, even considering the potential integration with passive optical networks as optical fronthaul, the final location of the splitters can be chosen. This low-rate communication link associated to PoF functionalities, could also be multiplexed with the ARoF link (blue line) shown in Fig. 1(a). PoF delivery uses 1 SMF and a 1×4 optical splitter at the RRH for accommodating the optical power to the different PV cells. In addition, an optical switch at the CO can share the HPL between different RRHs by using a RS232 over USB port communications as the interface with the PC controller.

All units feature generic external interfaces and a more detailed description is provided in further sections. An overview of the system specifications is given in Table I.

A. Central Office (CO)

The HPL at the CO is a Raman fiber laser at 1480 nm with a maximum power of 5 W and a wide linewidth to avoid Stimulated Brillouin Scattering that otherwise can affect the power delivery in the SMF [5]. The CO hardware (CO-HW) consists of two boards (Main and Communication board) based on low power MSP430 microcontroller with In-Circuit Serial Programming capabilities, a low speed communication interface for an optic fiber link (uplink and downlink), and one virtual UART interface over USB2.0. The USB interface is used for the communication between the CO-HW board and the software control based on a Matlab program and running on the PC. The commands generated on Matlab are sent to the remote side using the CO-HW as a gateway and a specific protocol is implemented based on a command-and-answer sequence. All devices have their own address. These elements of the CO are shown in the right side of Fig 2. The RRH parameters controlled and/or monitored by the CO are:

- input current sensor (CS)
- sensing parameters (temperature and humidity),
- percentage of charging battery,
- battery status (charging/discharging)
- control of energy management unit for either powering the load with PoF or charging the battery,
- configuration of two sleep mode scenarios (enter or awake):

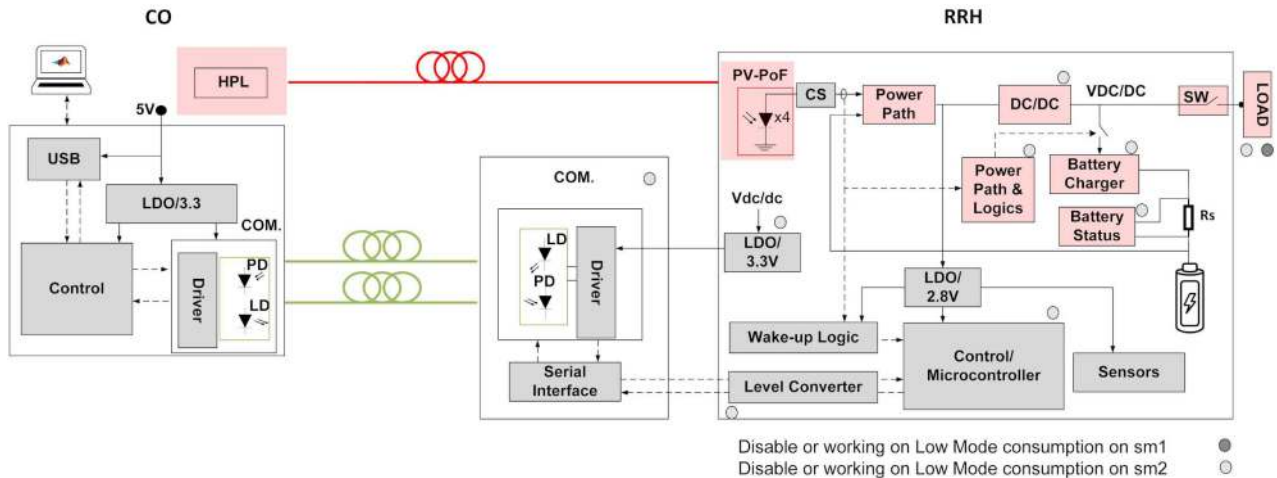


Fig. 2. Schematic of PoF system building blocks: Main and COM boards at CO and RRH side, including elements for sleep mode operation: •sm1, ◦sm2.

- sleep mode 1 (sm1): load is disconnected but RRH is listening through the communication channel,
- sleep mode 2 (sm2): minimum power consumption, the communication channel is also disconnected.

Apart from controlling capabilities on the RRH, the CO provides the optical power delivery for achieving electric powers of hundreds of mW at 14.43 km in SMF at RRH and switching control capabilities at CO.

B. Remote Receiver Unit as Part of RRH

The RRH hardware consist of two boards (Main and Communication board) controlled by a MSP430 microcontroller. The Main board includes an energy management unit with a DC/DC converter with the capability of tracking the maximum power point (MPPT) of the PV cells. The microcontroller translates a specific command received from the CO side to one of the following functionalities: enter into/exit of any of the two sleep modes, sensing a physical parameter (temperature and humidity), reading the battery status, enable of output voltage to the load. Every time that the microcontroller receives a command from the CO side, it generates a message with the requested parameters or one of the previous functionalities is executed. There are other capabilities such as: a real time clock (RTC) that works as a real time event log, battery backup to keep the load working 4.3 hours even without PoF energy, the generation of a regulated output voltage, the tracking of the maximum power point of the cells. When the RRH enters into sleep mode 2 (minimum power consumption), as there is no communications, a pulse from the HPL is used to awaken the RRH. A photograph of the implemented PCB of the Main board at the RRH is shown in Fig. 3, and includes the different elements shown on the schematic of Fig. 2. COM board for downlink and uplink communications is designed to minimize power consumption penalty at RRH, providing data rates of 6.6 kbits/s.

4 PV cells pigtailed to SMFs allow achieving 100 mW of electrical power for feeding the load, apart from the power required for the communications and control electronics to work at RRH. A single channel load switch, such as a N-channel MOSFET

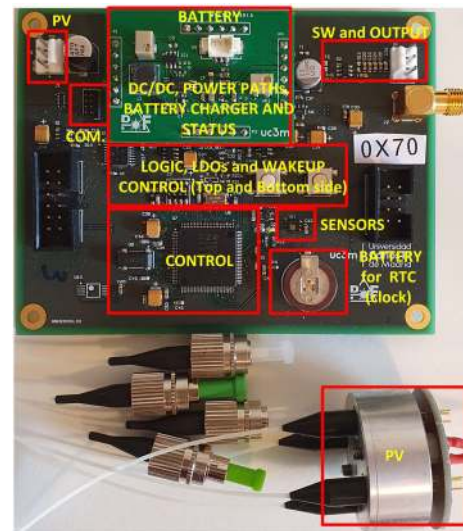


Fig. 3. Photograph of main elements of the RRH implemented: control, power stage and 4 PV cells within the heatsink. The communications board (COM) is not included.

SW TPS22810, operates within that power range (5 V 20 mA) and allows controlling the powering of the antenna RF power amplifier, a critical component for power modelling of any RRH [12], including the ARoF simplified RRH under discussion. This switch (SW) is embedded in the Main board. Finally, a specific heatsink is designed to avoid PV cells overheating, see Fig. 3.

III. EXPERIMENTAL SET-UP AND PERFORMANCE MEASUREMENTS

In 5G C-RAN deployments [13], either dedicated or shared scenarios can be considered meaning that the PoF power at 1480 nm can be sent in a dedicated fiber or can share the fiber by wavelength division multiplexing with the RoF signal, typically in the C-band. In our experiments, we are going to focus in providing the highest power at the RRH but avoiding any penalty in the efficiency of the system so initially a dedicated scenario

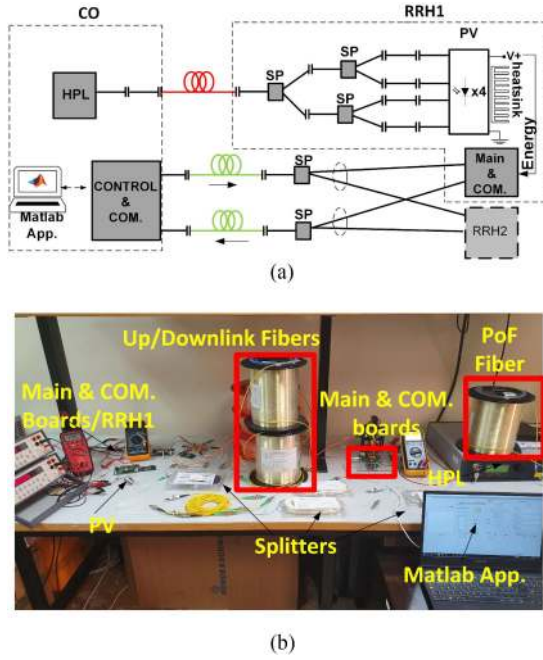


Fig. 4. Experimental set-up: (a) Schematic. (b) Photograph. HPL: High power laser, SP: Splitter, PV: Photovoltaic cells.

TABLE II
EXPERIMENTAL SET-UP POWER BALANCE DATA

1480 nm HPL input power (P_i)	+33.49 dBm (max s2*)
Optical fiber loss	3.89 dB (14.43km SMF)
Connector and splitters loss	0.82 dB
All 4 PV cells input power	+28.78 dBm

*s2: testing scenario 2 described in Section II.b.

is tested. The experimental set-up is shown in Fig. 4, including a schematic and a photograph.

A. Optical Power Budget Analysis and Non-Linear Effects

The optical power delivery system uses three spools of G652.D SMF, 2 of them for uplink/downlink communications.

A special analysis is devoted to the PoF link including HPL, around 14.43 km of SMF (14.429 km measured with OTDR), a 1×4 splitter made of two stages of 1×2 splitters in cascade, both able to handle a maximum power of 5 W. The HPL input power is adjusted to avoid exceeding the maximum power at each PV cell, being of 200 mW. All PV cells are connected to the RRH power stage. A summary of the losses of the PoF optical link are shown in Table II.

Regarding the non-linear effects, Stimulating Brillouin Scattering (SBS) has no influence when using broad HPL linewidths, greater than 10 GHz [5]. In this set-up, the PoF HPL has a Full Width Half Maximum (FWHM) greater than 2 nm.

On the other hand, Stimulating Raman Scattering (SRS) threshold power, P_{SRS} , is given by:

$$P_{SRS} = \frac{16 \cdot A_{eff}}{g_R \cdot L_{eff}} \quad (1)$$

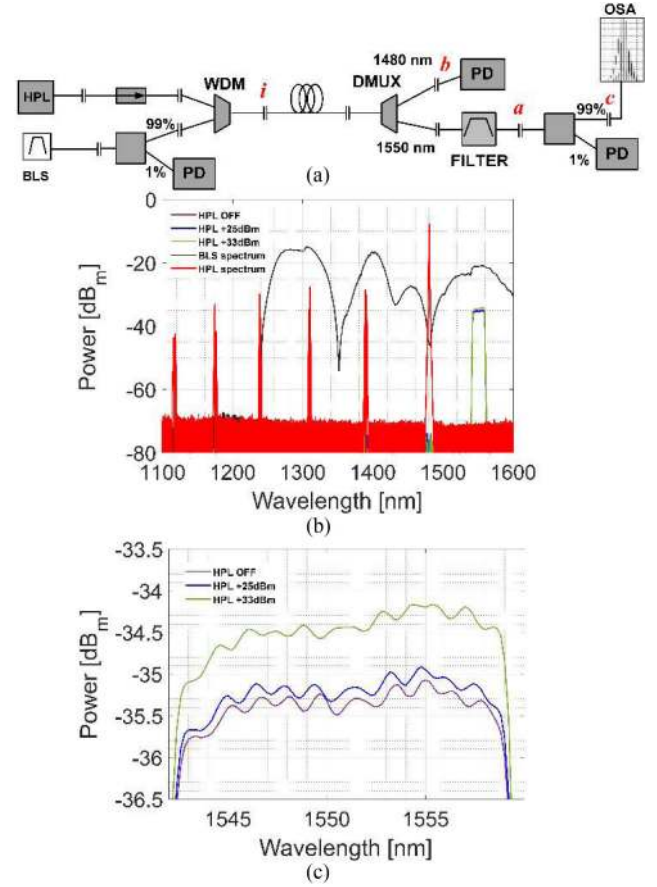


Fig. 5. (a) Experimental set-up. (b) Spectrum measurements: HPL/BLS and output power after 14.43 km SMF link at point c for different HPL powers. (c) Spectrum at point c , SRS effect analysis for different HPL powers. BLS: Broadband light source. WDM: Multiplexer. DMUX: Demultiplexer. OSA: Optical spectrum analyzer.

where g_R is the Raman gain coefficient, around $1 \cdot 10^{-13} \text{ m/W}$ ($1/2$ for non-polarized light) for silica. A_{eff} is the effective area and L_{eff} is the effective fiber length that depends on L and fiber attenuation coefficient, α as follows:

$$L_{eff} = \frac{1 - e^{-\alpha \cdot L}}{\alpha} \quad (2)$$

From Eqs. (1) and (2) considering a 14.43 km link of G652.D fiber at 1480 nm, P_{SRS} is around 0.8 W which is lower than the HPL input power used in our experiments. In [14] they suggest that after 5 km SMF the limiting effect on PoF delivery is SRS with a high impact; but they only calculate the P_{SRS} and not SRS in a real scenario, including the PV cell spectrum efficiency. Using VPI PhotonicsTM virtual photonic instrumentation software tool we estimate, in a dedicated scenario, the forward and backward SRS and the backward Rayleigh Scattering to verify if non-linear effects are more limiting than PV cells restrictions on the maximum power that the system can handle.

The measured attenuated spectrum of the Raman HPL, see Fig. 5(b), has low power levels in the C-band that are included in the simulations, as they can act as the SRS seed for the pumping at 1480 nm. Simulations show that for 2 W HPL input power mainly forward SRS reduces the power level at 1480 nm at the

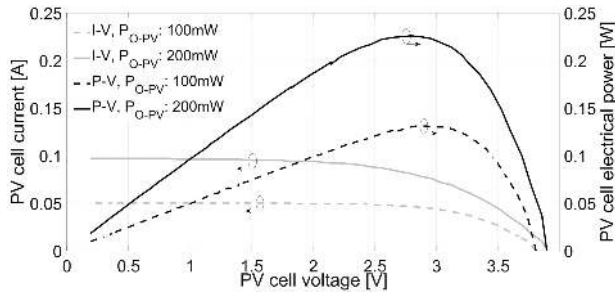


Fig. 6. Measurements of P-I and I-V curves of the 4 PV cells; for input optical powers of 100 mW and 200 mW per cell.

PV cells. But the impact on the system efficiency is small as SRS is within the PV cell spectrum from 1300 to 1600 nm. Both SRS and PoF at 1480 nm are converted to an electrical signal in the PV cells. The backscattered signal is around 6 dBm meanwhile forward signal in S+C band is around 30 dBm. For checking experimentally that most of the signal is in those bands when SRS is present, measurements in the set-up of Fig. 5(a) launching a HPL optical power of 980 mW, in a 14.43 km link along with an additional seed provided by a Broadband Light Source (BLS) were developed.

In Fig. 5(b), the low power of the BLS in the C-band is the SRS seed when pumping at 1480 nm with HPL input power higher than P_{SRS} . At the receiver side, there is a small amount of SRS filtered with a narrow C band filter (square shape signal). The measured spectrum at point *c* (see Fig. 5(a)), with the HPL output power configured OFF/+25/+33 dBm, is shown in a closer view in the Fig. 5(c). In the last case, SRS has more impact and the total power measured at 1480 nm DMUX output on the receiver site, point *b*, is of 190 mW. Meanwhile without the BLS, SMF link and C-band filter, just with the MUX/DMUX, the power at DMUX outputs is of 730 mW at 1480 nm and 3 mW at 1550 nm. The measurements show that the SRS effect is negligible as expected, as all S+C bands are collected at PV cells. But, in a shared scenario, SRS can play an important role as demultiplexers and a filter around the central wavelength of the 5G data signal is required [13]. In the shared scenario the noise of the HPL can be transferred to the data channel due to SRS, depending on the link length. This aspect has also to be taken into consideration.

B. Photovoltaic Cell +DC/DC Characterization

Fig. 6 shows the measured P-V and I-V curves of the 4 PV cells for input optical powers in each cell of 100 and 200 mW. The conversion efficiency is around 30% in all S+C bands with no overheating of the PV cells thanks to the heatsink shown in Fig. 3. The measured efficiency of the DC/DC converter with Maximum Power Point Tracking (MPPT) is 90%. Next section describes the peak consumption and power demand for the different scenarios.

C. Power Consumption Analysis and Sleep Mode Operation

The scenarios analyzed in terms of power consumption at the RRH are scenarios s1 and s2, being defined as:

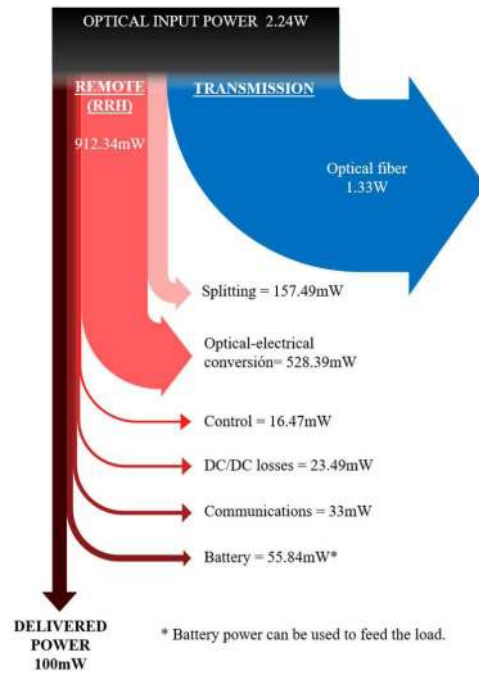


Fig. 7. Sankey diagram of the 14,43 km optical power link, starting with optical power input, PoF optical link power budget including transmission and power budget on remote receiver unit, including: splitting, optoelectrical conversion, uplink and downlink electrical power, final delivered electrical output power. The shown data represents the case of 100 mW delivered power at output voltage of 5 V with bidirectional data transmission over two optical links at a data rate of 6.6 kbits/s and charging battery with 11.167 mA at 4.2 V.

- s1: no load+charging battery with 11.167 mA at 4.2 V
- s2: 100 mW (5V 20 mA) load+ battery as in s1.

Apart from those scenarios there are two different sleep mode configurations presented in Section II.A. In all cases, the RRH operates at 4 MHz. The electrical power consumption of the communications board at 3.3 V with LD of 1310 nm OFF/ON is 3.3/33 mW respectively. Meanwhile the control electronics has a power consumption of 16.47 mW. Fig. 7 shows a modified Sankey diagram, following a similar analysis to that of reported in [15] but for the optical feeding power link, starting with the PoF optical link power budget (transmission) and remote receiver unit (RRH) power budget. This last one ranges from the optical splitting before PV cells to the final delivered electrical output power, and includes the optoelectrical conversion, the control and energy management, and the uplink and downlink COM electrical power. The calculations represent the case of 100 mW delivered power at the load with an output voltage of 5 V, a bidirectional data transmission over two optical fiber links at a data rate of 6.6 kbits/s and charging battery with 11.167 mA at 4.2 V. The largest fraction of this power is consumed on the optical fiber transmission and PV cells conversion efficiency, both with an efficiency close to 30% each. In the case of transmission, there is a reduced power consumption for fiber-optic links shorter than 14.43 km.

In the PV cells, state of the art efficiency at C band needs to be improved; at least to those levels achieved at 808 nm currently in used for short reach PoF systems [16], [17]. If we focus on

the electrical parts of the RRH, the largest used power is on battery charging, although this energy is not lost as it can be used afterwards to feed the load.

In the case of the RRH entering in any of the 2 sleep modes, there is a reduction in the power consumption at the remote site. Fig. 2 shows the different blocks that are switched off in each one of the sleep modes, sm1 (●) and sm2 (○). In any of them there is an energy saving. In sm1, the RRH is not able to feed any device but can listen and be awoken by software. In sm1, the RRH saves 111.11 mW, i.e., more than 50% of total RRH power. In sm2, the DC/DC is disabled and only the control unit with low power consumption mode operates at the RRH, consuming 5.86 mW, and can awake by hardware with a positive HPL pulse.

D. Functionality Tests and Discussion

In order to check the system functionality, different basic tests are defined and implemented using the software developed in Matlab. Those tests include at CO the fiber selection for power delivery by controlling the optical switch; displaying parameters at CO such as battery status or sensing parameters; controlling from CO (software/hardware) to make the RRH entering in and out of both sleep modes.

Tests also include sending data from RRH to CO and vice versa through the control channels; measuring power consumption in sleep modes and active node operation; battery charging through PoF channel until CO changes the configuration of the power stage. Considering the data described in previous sections, our system provides 226 mW with HPL optical power of 2.24 W, meaning an optical at CO to electrical RRH efficiency of 10% in 14.43 km optical power delivery using a SMF. In [14], they experimentally provide 107 mW with no overall efficiency, using a 17% single PV cell efficiency and they proposed using 8 nodes at 5 km with 50 mW in each nodes, but no measurements are reported. In [11], they launch 2.5 W optical power in the system and provide an electrical power of 190 mW using 4 PV cells in 8 km optical power delivery using a SMF, reaching an efficiency of 7.5%. Lower than in our case and at a shorter distance.

This system can be easily integrated in the PoF pooling concept described in [4] in a dedicated scenario.

As a summary, we provide a PoF system in a centralized RoF configuration with control management able to feed remote nodes at long distances, greater than 14.5 km, using SMF, with special functionalities. Those include powering some parts of low power consumption 5G RRHs and providing the capability of making those remote nodes to enter into sleep mode in idle periods reducing the overall power consumption of the system. We have proposed using HPL based on a Raman fiber laser with a broad linewidth to avoid SBS. Using a 1480 nm wavelength with link lengths and power levels at which SRS appears but still the penalty is affordable, without high backward SRS, and showing that PV cells can convert the whole range of wavelengths after SRS and provide energy enough to the system. The integration of all elements such as HPL, SMF, splitters, PV cells, with the specific electronics to make them work, showing the proposed functionalities. Including a low power consumption uplink. We have pointed out the impact of the different elements to provide

guidelines about the limitations and problems that can arise when increasing the power levels in those SMF fibers.

Main limitations of the reaching distance and remote power delivered on the proposed PoF system come from: a) the maximum input optical power that a PV cell can handle as well as its inherent efficiency value at 1480 nm, and b) the non-linear effects that arise in the optical fiber link when increasing the power level and link length, particularly SRS. Forward SRS is expected to have little impact on the overall PoF system efficiency as the operating PV cell spectrum ranges from 1300 to 1600 nm, still within the frequency shift imposed by SRS although some efficiency variations are expected. However, the negative impact of backward SRS may be on a greater extent, even not acceptable in some PoF use-cases, if longer links and higher injected optical powers are planned. The need of more PV cells (and so splitting stages) as well as the increasing influence of non-linear effects, respectively, penalize the net PoF system efficiency. Finally, in our current system able to provide the functionality of centralized control of RRH, including the sleeping/awaking of the RRHs, the need of the uplink with low power consumption also poses a limitation in the system. The current uplink design looks for a minimum impact on the overall RRH power consumption, with a low-speed data rate and the RRH laser diode operation near its threshold current. In the uplink, the signal goes through a splitter that increases the losses. It works at 6.6 kbits/s and consumes 33 mW but the maximum link length is limited by the power budget. Independently of the final use of PoF either to fully power a low power consumption 5G RRH, a potential evolution of [18]–[19], or to partially power some critical elements [20] and control the on/off switching of some RRH parts in idle periods to improve energy efficiency, different communications channels can be considered. This PoF system can provide a minimum energy in an independent way allowing connectivity for instance in areas where you want to have a special security or on rural areas where some specific critical infrastructures need a good coverage and special protection against natural disasters. This technology provides the operator with a direct control of the infrastructure, even as a back-up system. In our current design, low-power consumption oriented, there is a channel with low bit rates for independently controlling the power consumption of the remote node. Deviating around 1/3 of the total power delivered to the RRH for powering it. Future higher bit rate designs compliant with low latency 5G networks integrating the control of the data channel itself can consume around 1 W. Meaning that if only 1/3 of the RRH power is used for communications around 3 W will be provided to the 5G node. This implies around 10 W of optical power at the CO or 4 HPLs with 2.5 W each of input power at each SMF for avoiding high SRS backscattering impact. So the feeding capability can be increased by using SMF bundles with higher PoF levels at CO with more HPLs or using different cores of MCF while avoiding non-linear effects [5], [13].

In the following, we describe an example of potential power saving, when using the strategy of activating different sleep modes. We consider the power modeling data provided in [12], where the power amplifier consumes around 30% of total power and being the RRH power consumption of our system negligible,

there can be an overall saving of 18% if keeping sm1 at night and sm2 during 10% of day hours. This can be further improved by reducing optical power transmission to the required values for only providing sm1 and sm2 operation. The independent sleep modes provided by the PoF solution contribute to the efforts of improving the energy efficiency and minimizing CO₂ emissions of future mobile networks [21].

IV. CONCLUSION

PoF in a centralized configuration compatible with a C-RAN architecture using SMF bundles and including sleep mode capabilities is experimentally verified. A single SMF feeds with 226 mW at 14.43 km for controlling and switching ON/OFF some parts of low power RRHs by launching 2.24 W. Additional functionalities include sleep mode operation, battery charging and sensing. Stimulated Raman Scattering contributes to final electrical power conversion at the receiver. The system includes low power consumption bidirectional communication with two SMFs used by 2 RRHs. There is an overall 10% efficiency from optical power at CO to electrical power at RRH. Specific heatsink designs for avoiding PV cell overheating are included. The system is scalable using bundles of SMFs and HPLs providing higher power level for feeding communication channels at higher data rates. Future 5G networks will require low power consumption RRHs and strategies to reduce carbon footprint where control and feeding from the operator size, as the system proposed in this paper, can be very helpful.

ACKNOWLEDGMENT

The authors thanks X. Barreiro for his work in designing the heatsink of the PV cells and F.M.A. Al-Zubaidi in simulating SRS with VPI PhotonicsTM.

REFERENCES

- [1] C. Liu *et al.*, "A novel multi-service small-cell cloud radio access network for mobile backhaul and computing based on radio-over-fiber technologies," *J. Lightw. Technol.*, vol. 31, pp. 2869–2875, 2013.
- [2] L. Bogaert *et al.*, "36 Gb/s narrowband photoreceiver for mmWave analog radio-over-fiber," *J. Lightw. Technol.*, vol. 38, no. 12, pp. 3289–3295, Jun. 2020, doi: [10.1109/JLT.2020.2968149](https://doi.org/10.1109/JLT.2020.2968149).
- [3] Z. Tan, C. Yang, and Z. Wang, "Energy evaluation for cloud RAN employing TDM-PON as front-haul based on a new network traffic modeling," *J. Lightw. Technol.*, vol. 35, no. 13, pp. 2669–2677, Jul. 2017, doi: [10.1109/JLT.2016.2613095](https://doi.org/10.1109/JLT.2016.2613095).
- [4] G. Otero *et al.*, "SDN-based multi-core power-over-fiber (PoF) system for 5G fronthaul: Towards PoF pooling," in *Proc. 44th Eur. Conf. Opt. Commun.*, Rome, 2018, pp. 1–3.
- [5] C. Vázquez *et al.*, "Multicore fiber scenarios supporting power over fiber in radio over fiber systems," *IEEE Access*, vol. 7, pp. 158409–158418, Oct. 2019, doi: [10.1109/ACCESS.2019.2950599](https://doi.org/10.1109/ACCESS.2019.2950599).
- [6] A. P. Goutzoulis, J. M. Zomp, and A. H. Johnson, "Development and antenna range demonstration of an eight-element optically powered directly modulated receive UHF fiberoptic manifold," *J. Lightw. Technol.*, vol. 14, no. 11, pp. 2499–2505, Nov. 1996.
- [7] M. Matsuura, N. Tajima, H. Nomoto, and D. Kamiyama, "150-W power-over-fiber using double-clad fibers," *J. Lightw. Technol.*, vol. 38, no. 2, pp. 401–408, Jan. 2020, doi: [10.1109/JLT.2019.2948777](https://doi.org/10.1109/JLT.2019.2948777).
- [8] R. Muñoz *et al.*, "Experimental demonstration of advanced service management in SDN/NFV front-haul networks deploying ARoF and PoF," in *Proc. Eur. Conf. Opt. Commun.*, 2019, pp. 459–463.
- [9] S. Rommel *et al.*, "Towards a scaleable 5G fronthaul: Analog radio-over-fiber and space division multiplexing," *J. Lightw. Technol.*, vol. 38, no. 19, pp. 5412–5422, Oct. 2020, doi: [10.1109/JLT.2020.3004416](https://doi.org/10.1109/JLT.2020.3004416).
- [10] I. Tafur *et al.*, "Space division multiplexing 5G fronthaul with analog and digital radio-over-fiber and optical beamforming- the blueSPACE concept," pp.1–15, Aug. 2018, doi: [10.5281/zenodo.1403140](https://doi.org/10.5281/zenodo.1403140).
- [11] C. Diouf *et al.*, "Design, characterization, and test of a versatile single-mode power-over-fiber and communication system for seafloor observatories," *IEEE J. Ocean. Eng.*, vol. 45, no. 2, pp. 656–664, Apr. 2020, doi: [10.1109/JOE.2018.2876049](https://doi.org/10.1109/JOE.2018.2876049).
- [12] B. Debaillie, C. Desset, and F. Louagie, "A flexible and future-proof power model for cellular base stations," in *Proc. IEEE 81st Veh. Technol. Conf.*, 2015, pp. 1–7, doi: [10.1109/VTCSpring.2015.7145603](https://doi.org/10.1109/VTCSpring.2015.7145603).
- [13] C. Vázquez, D. S. Montero, F. Al-Zubaidi, and J. López-Cardona, "Experiments on shared and dedicated power over fiber scenarios in multicore fibers," in *Proc. 28th Eur. Conf. Netw. Commun. (EuCNC)*, 2019, pp. 412–415.
- [14] L. Ma, K. Tsujikawa, N. Hanzawa, and F. Yamamoto, "Design of optical power delivery network based on power limitation of standard single-mode fiber at a wavelength of 1550 nm," *Appl. Opt.*, vol. 54, no. 12, pp. 3720–3724, 2015.
- [15] H. Helmers, C. Armbruster, M. von Ravenstein, D. Derix, and C. Schöner, "6-W optical power link with integrated optical data transmission," *IEEE Trans. Power Electron.*, vol. 35, no. 8, pp. 7904–7909, Aug. 2020.
- [16] J. D. López-Cardona, C. Vázquez, D. S. Montero, and P. C. Lallana, "Remote optical powering using fiber optics in hazardous environments," *J. Lightw. Technol.*, vol. 36, no. 3, pp. 748–754, Feb. 2018, doi: [10.1109/JLT.2017.2776399](https://doi.org/10.1109/JLT.2017.2776399).
- [17] J. D. López-Cardona, D. S. Montero, and C. Vázquez, "Smart remote nodes fed by power over fiber in Internet of Things applications," *IEEE Sensors J.*, vol. 19, no. 17, pp. 7328–7334, Sep. 2019, doi: [10.1109/JSEN.2019.2915613](https://doi.org/10.1109/JSEN.2019.2915613).
- [18] T. Umezawa, P. T. Dat, K. Kashima, A. Kanno, N. Yamamoto, and T. Kawanishi, "100-GHz radio and power over fiber transmission through multicore fiber using optical-to-radio converter," *J. Lightw. Technol.*, vol. 36, no. 2, pp. 617–623, Jan. 2018, doi: [10.1109/JLT.2017.2731991](https://doi.org/10.1109/JLT.2017.2731991).
- [19] "5g connected stadiums – seamless experience". [Online]. Available: <https://www.ericsson.com/en/small-cells/stadium> (Accessed May 20, 2021).
- [20] F. M. A. Al-Zubaidi, J. D. López-Cardona, D. S. Montero, and C. Vázquez, "Optically powered radio-over-fiber systems in support of 5G cellular networks and IoT," *J. Lightw. Technol.*, 2021, to be published, doi: [10.1109/JLT.2021.3074193](https://doi.org/10.1109/JLT.2021.3074193).
- [21] "Nokia confirms 5G as 90 percent more energy efficient | nokia." [Online]. Available: <https://www.nokia.com/about-us/news/releases/2020/12/02/nokia-confirms-5g-as-90-percent-more-energy-efficient/> (Accessed: Mar. 15, 2021).

Juan Dayron López-Cardona received the M.Sc. degree in electronic systems engineering from the Universidad Carlos III of Madrid (UC3M), Spain, in 2016, where he is currently working toward the Ph.D. degree. His research interests include low power electronics, multicore optical fibers, and power over fiber systems.

Rubén Altuna received the M.Sc. degree in electronic systems engineering from the Universidad Carlos III of Madrid, Spain, in 2020. His research interests include radio over fiber, instrumentation systems, and power over fiber systems.

David Sánchez Montero received the Ph.D. degree from the Universidad Carlos III of Madrid (UC3M), Spain, in 2011. He is currently an Associate Professor with Electronics Technology Department, UC3M. His current research interests include fiber-optic sensors, multicore optical fibers, WDM-PON networks, and power over fiber systems.

Carmen Vázquez (Senior Member, IEEE) is currently Full Professor with Electronics Technology Department, Universidad Carlos III of Madrid, Spain. She was with TELECOM, Denmark, and Telefónica Investigación y Desarrollo, Spain. Her research interests include integrated optics, optical communications and instrumentation with plastic and multicore optical fibers, fiber optic sensors, power over fiber, and WDM-PON networks. She is also a Fellow member of SPIE.